The Integrated Carbon Dioxide Removal, Compression, and Storage (CRCS) System

Tra-My Justine Richardson[1]
Logyx LLC, Mountain View, CA, 94043, USA

Jason Samson[2], Gary Palmer[3], Brian Koss[2], Grace Belancik[4], John Hogan[4]
NASA, Moffett Field, CA, 94035

Roger Huang[5]
KBRWyle, Moffett Field, CA, 94035

James Knox[6]
NASA Marshall Space Flight Center, Huntsville, Alabama, 35812, USA

and

Darrell Jan[4]
NASA, Moffett Field, CA, 94035

The Carbon Dioxide Removal, Compression, and Storage (CRCS) system was designed to remove carbon dioxide ($CO_{2(g)}$) from the spacecraft cabin atmosphere and compress and store the $CO_{2(g)}$ for further processing. Previous conference papers describe the hardware design and functional testing of the single and dual beds. This paper discusses the integrated system test results when dry $CO_{2(g)}$ latent air (2600ppm $CO_{2(g)}$) enters the system at 30 SCFM.

I. Nomenclature

4BMS = 4-Beds Molecular Sieves
4BMS-X = 4-Beds Molecular Sieves Exploration
AC-TSAC= Air Cooled Temperature Swing Adsoption and Compression
AES = Advanced Exploration System
ARC = Ames Research Center
ARS = Air Revitalization System
BaRDD = Bulk and Residual Dryers Downselect
CDRA = Carbon Dioxide Removal Assembly
CMS = Carbon Management System
$CO_{2(g)}$ = Carbon Dioxide Gas
CRCS = Carbon Dioxide Removal Compression and Storage
ISS = International Space Station
LPCOR = Low Power Carbon Dioxide Removal
MFC = Mass Flow Controller
MSFC = Marshall Space Flight Center
NASA = National Aeronautics and Space Administration

[1] Research Engineer/Scientist, Bioengineering, Mailstop 239-15
[2] Mechanical Engineer, Bioengineering, Mailstop 239-15
[3] Machinist, Bioengineering, Mailstop 239-15
[4] Physical Scientist, Bioengineering, Mailstop 239-15
[5] Research Engineer Technician, Bioengineering, Mailstop 239-15
[6] Aerospace Engineer, Environmental Control and Life Support Development Branch/ES62.

PSA = Pressure Swing Adsorption
RTD = Resistance Temperature Detectors
SCFM = Standard Cubic Feet per Minute
SPFD = Simplified Process Flow Diagram
TC-TSAC = Thermally Coupled Temperature Swing Adsoption and Compression
TSAC = Temperature Swing Adsoption and Compression
UHP = Ultra High Purity
WC-TSAC = Water Cooled Temperature Swing Adsoption and Compression

I. Introduction

THE National Aeronautics and Space Administration (NASA) Temperature Swing Adsorption Compression (TSAC) is a solid-state Carbon Dioxide (CO_2) compressor that compresses, stores, and delivers $CO_{2(g)}$ as needed to downstream processes. The TSAC concept was first proposed as in-situ propellant production by capturing $CO_{2(g)}$ from the Martian atmosphere and converting it to methane [1-3]. The Ames Research Center (ARC) Air Revitalization group has been working on different TSAC technologies for use in the Martian atmosphere as well in life support function on manned spaceflight. The details of these researches are well documented in various conference papers[4-6].

A. A Brief Background

The Carbon Dioxide Removal, Compression, and Storage (CRCS) system was initially designed as a $CO_{2(g)}$ removal and compression component of the Low Power Carbon Dioxide Reduction (LPCOR) system [5-8]. The LPCOR system consists of the water removal component and the $CO_{2(g)}$ removal and compression component. Water must be removed first because the $CO_{2(g)}$ sorbent will adsorb both water and $CO_{2(g)}$. The water removal section used Nafion hollow fiber membranes to remove 80% of the water from cabin air and the NovelAire system to remove the remaining 20%. Dry $CO_{2(g)}$ latent air then enters the CRCS system.

The CRCS system has two functions: (1) adsorb $CO_{2(g)}$ from cabin air; (2) compress and store $CO_{2(g)}$ for delivery as needed to downstream processes. The water removal component of the LPCOR was eliminated for further development as a result of the Bulk and Residual Dryers Downselect (BaRDD) downselect activities in 2013[9]. The CRCS was developed individually as the $CO_{2(g)}$ removal and compression unit. The CRCS is similar in function to the 4-Bed Molecular Sieve (4BMS) $CO_{2(g)}$ adsorbent bed combined with the $CO_{2(g)}$ mechanical compressor currently in operation on the International Space Station (ISS), Figure 1.

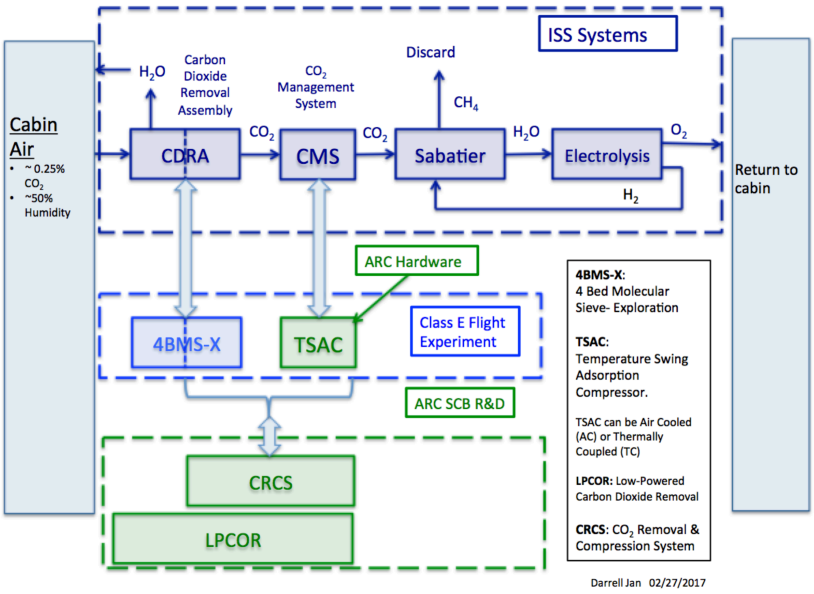

Figure 1: A picture showing the different functions of the various Air Revitalization System components on ISS and those being developed at ARC.

Previous CRCS papers discussed the design, fabrication, and preliminary testing of a single and dual test canisters[10, 11]. Here, the final development efforts and testing results of the integrated CRCS (2-beds system) are discussed. The CRCS test results presented here were presented at a $CO_{2(g)}$ Removal system gate review at the end of 2016. The CO_2 gate review looked at the various NASA funded $CO_{2(g)}$ removal technologies: The Pressure Swing Adsorption (PSA) system developed at the University of South Carolina; the 4-BMS-X system; the liquid amines system; and the CRCS system. Details of the CRCS gate review are discussed in the Results and Discussion Section of this paper.

B. The Process Flow Diagram

For a TSAC system, the $CO_{2(g)}$ is adsorbed onto the sorbent and the $CO_{2(g)}$ is desorbed by heating the sorbent to a target temperature. Figure 2 shows a Simplify Process Flow Diagram (SPFD) for the integrated CRCS system. The system consists of two concentric cyclinders. Stage 1, the internal cylinder, adsorbs the $CO_{2(g)}$ from cabin air; Stage 2, located in the outer annulus, compress and store the $CO_{2(g)}$. The valves embedded in the lids open Stage 1 to allow air input into stage 1 and close during vacuum and heating operations. Valves between stage 1 of one unit and stage 2 of the next unit open and close when stage 1 pressure is higher than stage 2 pressure. The uniqueness of this concentric design is the shared wall between the stage 1 and stage 2. Here, as stage 1 is heated, stage 2 is also heated. This leads to a decrease in total system power. Using the numbering system in Figure 2, the $CO_{2(g)}$ process flow for a half-cycle is described in Table 1.

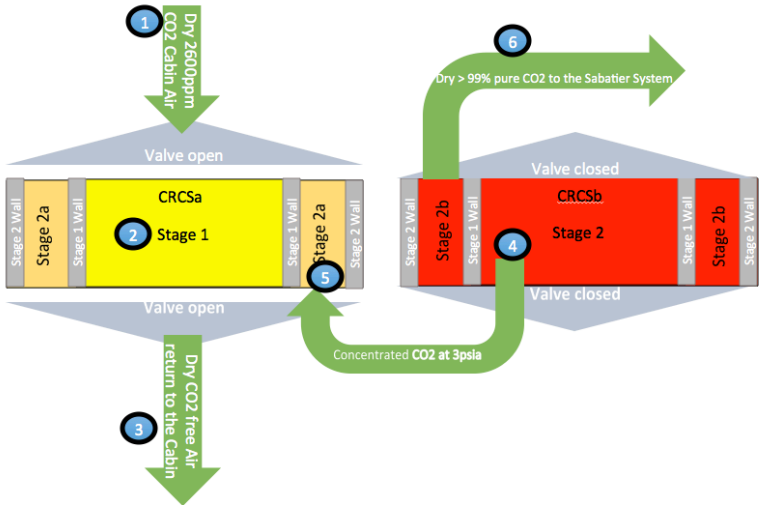

Figure 2: The Simple Process Flow Diagram (SPFD) for the integrated CRCS system.

Table 1: A table describing the $CO_{2(g)}$ flow for a half-cycle based on the numbering of the SPFD in Figure 2

Stage 1A CO_2 adsorption	**#1**: Dry $CO_{2(g)}$ latent (2600ppm) air enters CRCS-A Stage 1 **#2:** In stage 1A, the 13X sorbent absorbs the $CO_{2(g)}$ **#3:** The $CO_{2(g)}$ free air exit into the room.
Stage 1B desorption and stage 2B CO_2 adsorption	**#4:** Stage 1B heats to deliver concentrated $CO_{2(g)}$ to stage 2A **#5:** Stage 2A adsorbs the concentrated $CO_{2(g)}$
Stage 2B CO_2 delivery	**#6:** as CRCS-B stage 1 is heated, stage 2B is also heated and dry concentrated $CO_{2(g)}$ is output to the hood (or to the Sabatier System).
The second half cycle starts by CRCS-A and CRCS-B roles reversing.	

II. System Design

The CRCS development efforts took into consideration both the water-cooled and the air-cooled TSAC (AC-TSAC) systems test results. The AC-TSAC is a dual-bed system so when one bed is adsorbing, the other is desorbing. Figure 3 shows the AC-TSAC 2000 producing $CO_{2(g)}$ at 4kg/day. The vertical lines indicate the $CO_{2(g)}$ product flow switching from one bed to another. The goal of the CRCS design is to replicate this $CO_{2(g)}$ compression and delivery feature of the AC-TSAC 2000 and add the $CO_{2(g)}$ adsorption feature of the 4BMS currently in operation on ISS. A summary of the CRCS design rational are discussed below.

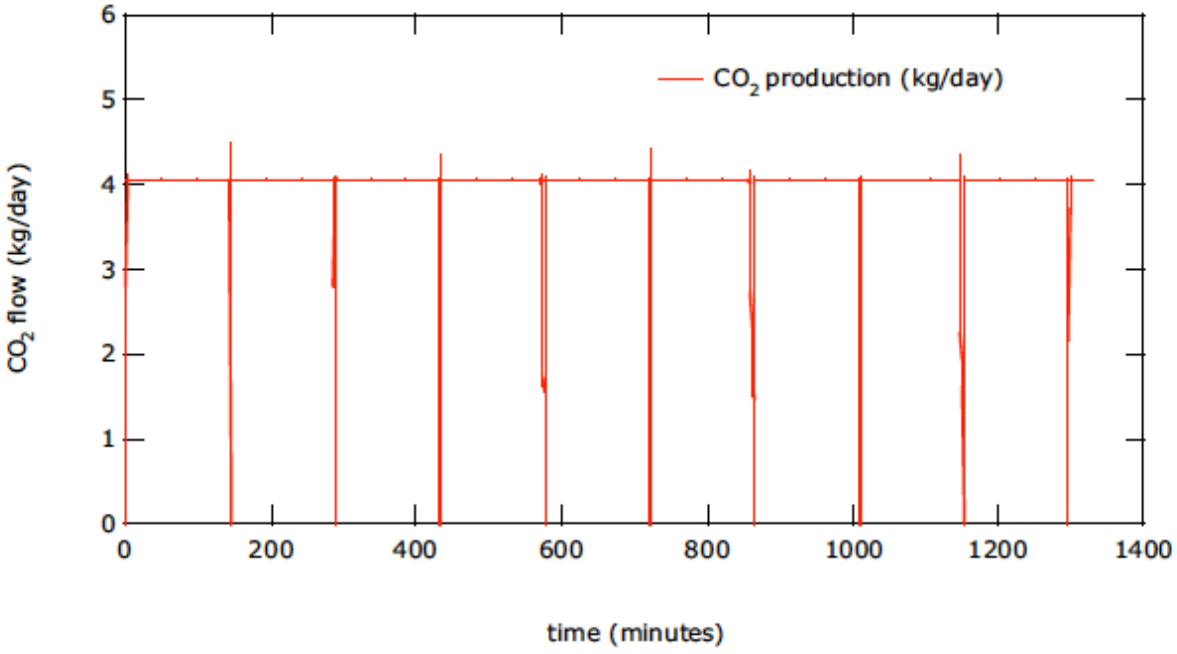

Figure 3: $CO_{2(g)}$ flow results for the AC-TSAC-2000[6].

C. Mechanical Design

Each AC-TSAC-2000 bed is a rectangular aluminum canister, **Figure 4**(a). Therefore, the first iteration of the CRCS design consists of rectangular canisters, **Figure 4**(b). A smaller canister performs the TSAC function and is embedded inside a larger one. It was determined that the regtangular design would not be a mass efficient design under the operating pressure conditions. Therefore, the final CRCS design consists of two concentric cyclinders, **Figure 5**. The concentric design would allow up to 28psig operating pressure and allow flow uniformity within stage 1.

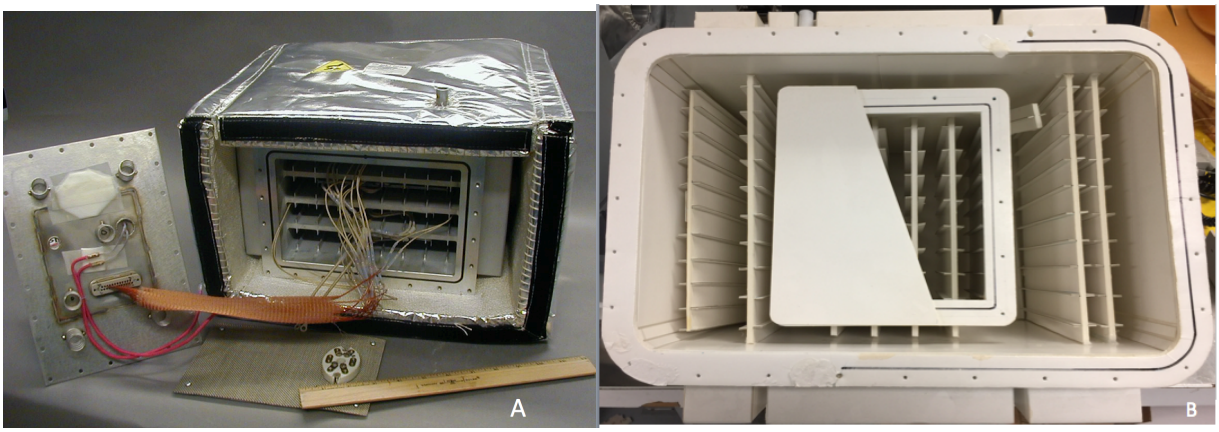

Figure 4: (a) The AC-TSAC 2000; (b) A model of the CRCS rectangular design

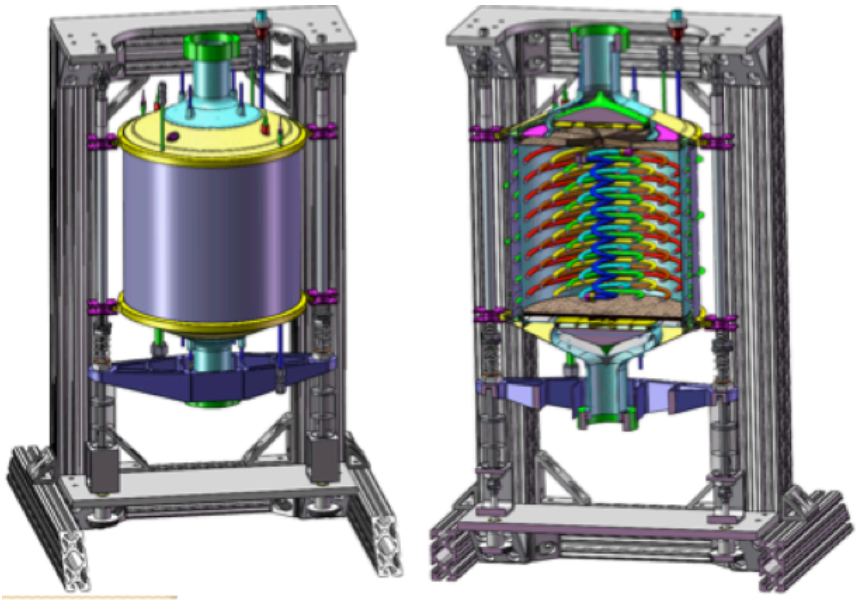

Figure 5: A Solidwork image of the CRCS showing the outside wall and the internal heaters configuration the CRCS rack 3D models and the fully assembled test system.

In an effort to reduce mass, volume, and power and to accommodate the expected 300˚C regeneration temperature, the CRCS canisters were fabricated with thin 316 stainless steel walls and embedding the stage 1 valves in the canister lids. The CRCS walls was fabricated as thin possible (0.028" for stage 1 and 0.025" for stage 2), but thick enough to be able to withstand up to 28psig. The pneumatically operated valves are thin circular stainless steel plates. Kalrez high temperature O-rings covers the rim of the plates to seal the lids with the valve when needed during operation. As the circular plates lifts, the valves is in the open position and air can enters stage 1. **Figure 6** shows the final design of the CRCS canister lid with the valve plate in the center. **Figure 7** shows the dual-beds SolidWorks model and the assembled canisters on the rack.

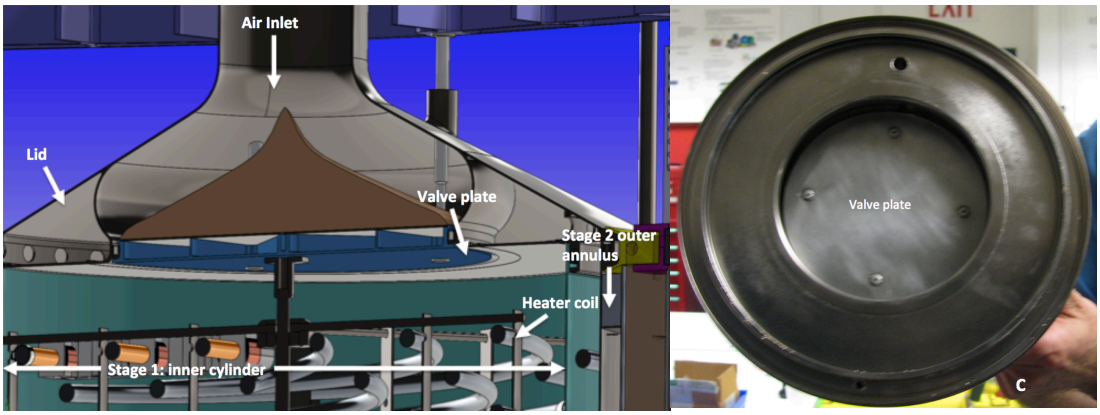

Figure 6: (left) SolidWork model cross section showing the valve plate; (right) a picture of the fabricated lid with the valve plate in the middle

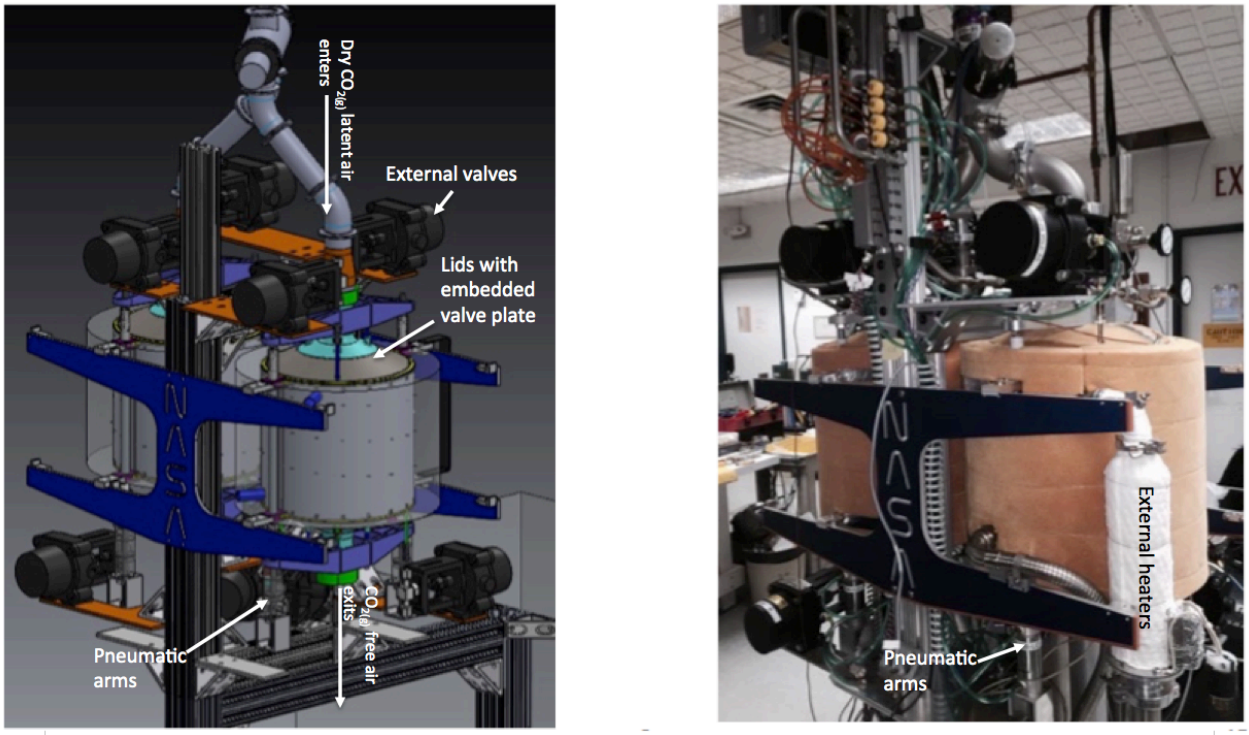

Figure 7: (left) the Solidwork model for the integrate CRCS; (right) the assembled CRCS.

D. System Specification

The CRCS was designed to maintain the ISS cabin air $CO_{2(g)}$ concentration at 2600ppm and deliver concentrated $CO_{2(g)}$ to the Sabatier system as needed at 20 psia. The design parameters are listed in **Table 2**.

Initially, stage 1 sorbent was the 5A zeolite. However, based on sorbent evaluation test done at Marshall Space Flight Center (MSFC), the Grace Davidson 544 13X were used instead.

Moate et. al.[12] showed that at 300˚C, the 5A $CO_{2(g)}$ working capacity increases and more $CO_{2(g)}$ is desorbed into stage 2. However, above 250˚C, feasibility overrode optimal system performance since system components (e.g. valves, o-rings, gaskets, pressure transducers, etc.) were costly and lead times were long. Given that the 13X material does not require a high regeneration temperature, the final CRCS system configuration were designed such that 280˚C (the 13X zeolite regeneration temperature) is the highest regeneration temperature.

The 35µm and the 180µm screens were used to distribute the flow evenly as well as sorbent containment. The TechMat were used for dust containment.

The Solidmide insulation were chosen due to its light weight and high thermal capacity. The blower were set at 20SCFM to coincide with the current blower capacity available on ISS. The cooling jackets were custom fabricated thin Stainless Steel metal sheets that were welded to form hollow cyclinders. These cyclinders were wrapped around the stage 2 outer wall.

Based the total bed volumes and subtracting the internal components, the total estimated sorbent mass for stage 1 and 2 are 9.48lb_m and 2.37lb_m respectively.

Table 2: The final CRCS specification table.

	Stage 1	Stage 2
Number of Crew members	4	
Inlet CO2 concentration, ppm	2600	
CO_2 removal efficiency, %	85	
Material of construction	SS 316	
Canister shape	Concentric Cylinders	
CO_2 input concentration	2600ppm	>99%
Canister total empty volume, L	12	2.77
CO_2 delivery pressure, psia	3	20
Adsorbent size and shape		UOP 5A-MG-16X40
Adsorbent mass, lb_m(kg)	(20.86) 9.48	5.21(2.37)
Adsorbent density, g/cc	0.79	
Sorbent volume		
Void space, L	0.67	0.27
Heaters capacity, W	1249	422.94
Regeneration temperature, ˚C	250	250
Bake out temperatures, ˚C	280	280
Number of heater coils	6	1
# of 2-wire RTDs on heater coils	6	2
# of 2-wire RTDs in adsorbent material	12	3
Cooling jacket	SS316 sheet : ¼" gap	
Blower, SCFM	20	
Insulation	High Performance SOLIMIDE Polyimide Foam Insulation (2" on the side walls and 1 ¾" on the top and bottom lids)	
Screens on the top	Super-Small Particle-Filtering Stainless Steel Wire Cloth, Woven, 316 Stainless Steel, 50x250 (35 microns) Mesh.	
Screens on the bottom	Super-Small Particle-Filtering Stainless Steel Wire Cloth, Woven, 316 Stainless Steel, 50x250 (35 microns) and 80 x 700 (180 microns)Mesh	
Fabric Screen used for sorbent containment	¼" Low Density Techmat	

III. Temperature Uniformity

Previous publications showed results for testing the temperature uniformity in CRCSa and as well as preliminary integrated testing of both the CRCSa and CRCSb [10, 11]. These test results showed that the spiral heater coils yield uneven temperature distribution both in the axial as well as the radial direction[10]. The lack of temperature uniformity inside the beds were due to the following:

1. The heat lost to the top and bottom lids due to metal to metal contact between the container walls and the lids.
2. The heater coils were fabricated with the same resistance throughout the length contributing to the "oven effect" where the center were hotter than the outer ends.
3. In stage 1, the six heater coils were not individually controlled because the lids were fabricated with a limited number of power feedthroughs.
4. The canister mounting arms were not thermally isolated so the aluminum mounting plates acted as heat sinks.

Given the constrains of the prefabricated hardware, efforts were made to examine different ways to improve temperature uniformity within stage 1. One, there is only one power feedthrough in the lid to control the six stage 1 heater helixes. The lids were fabricated with thin stainless steel walls and the air gaps were vacuum sealed. Therefore, there is a high risk of damaging the lids if additional power feedthroughs were welded on. Two, the heater coils were custom fabricated cartridge heaters with uniform resistance throughout the length at a specified diameter such that the coils could be evenly spaced throughout the canister. Three, there were not enough space at the top or the bottom of the canister to add additional heaters to make up for the heat lost at the top and the bottom. As a result, efforts were made to look at arranging the six helical heaters in various series and parallel configurations to examine if temperature uniformity was achieved. It did not.

Additionally, tests were done by placing resistors at the heater connector ends. There were improvements, but the heat generated by the resistors themselves were creating hot spots. Given these options, the final conclusion was to add an external heater to the heating/cooling jacket loop to assist in heating stage 2 and possibly improve the temperature distribution in the radial direction. This external heater, see Figure 7, is an added component for the proof of concept system, but would not be added to the optimal design. Given prefabricated hardware and no workable solution to the lack of temperature uniformity, the integrated tests used the heaters coils as is.

IV. Methods

After assembly, the integrated CRCS system were tested through adsorption and desorption 60-minutes half-cycles according to the work cycle in Figure 8 and Table 3. After adsorption, vacuum is pulled in stage 1 to remove any residual air or contaminant left in the canister. After stage 1 delivers $CO_{2(g)}$ to stage 2 of the opposite canister, it is placed in standby so that the system can be synchronized with the AirSave mode of the 2nd canister.

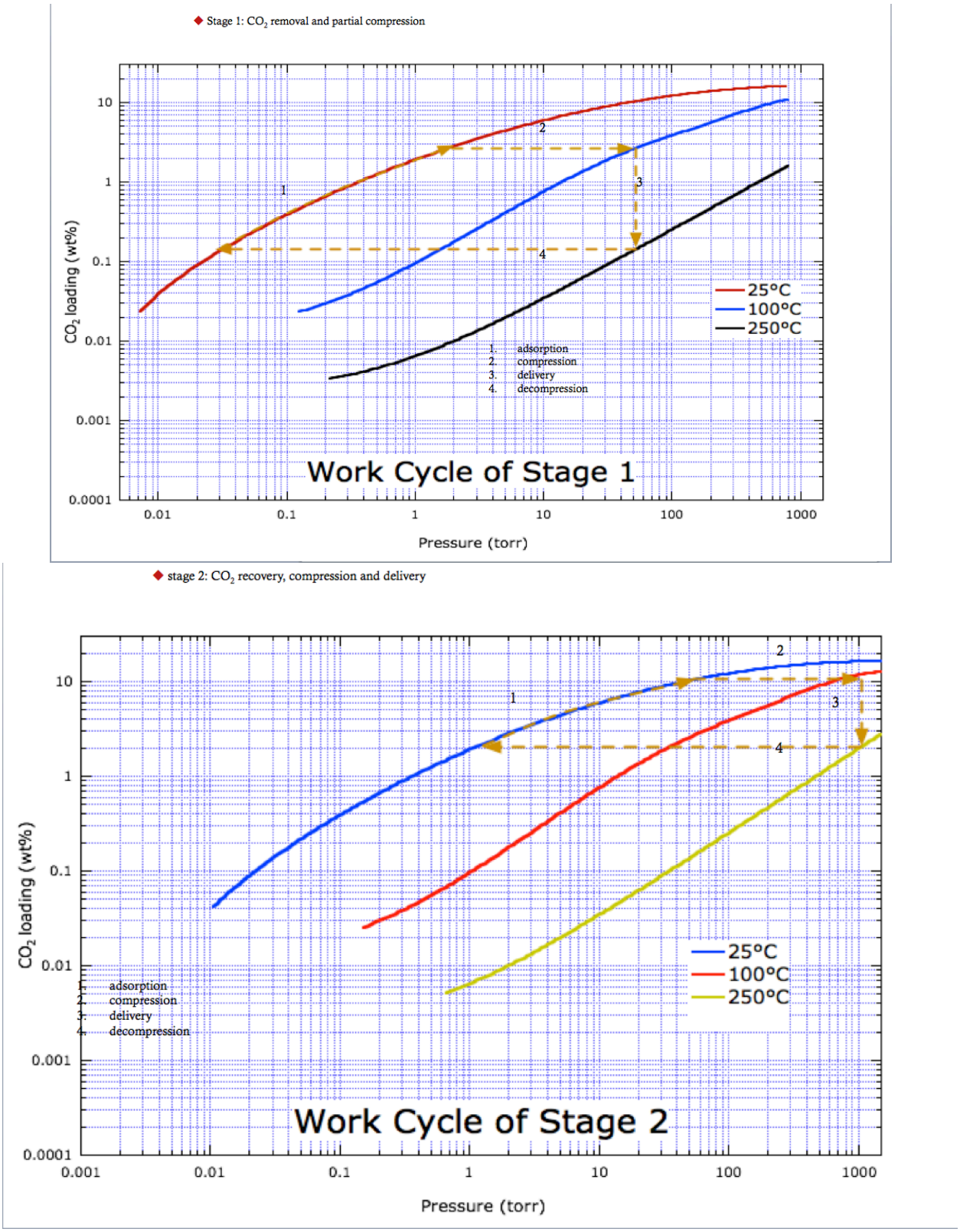

Figure 8: The graphs showing the work cycle for CRCS stage 1 and stage 2[4].

Table 3: A table outlining the CRCS beds operation during the 120-minutes full cycle.

Cycle times		0-49 minutes	50-60 minutes	61-109 minutes	110-120 minutes
CRCS-A	Stage 1A	CO2 Adsorption from Cabin Air	AirSave	CO2 delivery to Stage 2B (Heating)	Stanby
	Stage 2A	CO2 Adsorption from Stage 1B	Heating	Compression and Delivery to the Sabatier(Heating)	
CRCS-B	Stage 1B	CO2 delivery to Stage 2A (Heating)	Stanby	CO2 Adsorption from Cabin Air	AirSave
	Stage 2B	Compression and Delivery to the Sabatier (Heating)		CO2 Adsorption from Stage 1A	Heating

A. Sorbent preparation

Before loading, the both the 13X and 5A sorbents were baked-out in bake-out canisters in an oven with Ultra High Purity (UHP) nitrogen sweep gas (Matheson Tri-Gas). The oven baked out followed the ramp (2˚C/min) and soak oven bake-out steps: 50˚C for 1 hour; 100˚C for 2 hours; 350˚C until the outlet dewpoint is lower than -70˚C. After oven baked-out, the bake-out canisters were sealed to prevent the sorbent from re-adsorbing water. The baked-out sorbent were then loaded onto the CRCS beds as quickly as possible with UHP nitrogen sweep gas flowing through the CRCS beds. Once loaded, the sorbents were then baked-out in place following the same ramp and soak steps as the oven bake-out procedure with the exception that the final ramp temperature is only 280˚C instead of the 350˚C. 280˚C is used because the CRCS assembly was not designed for temperatures above 300˚C. The in-place bake out continued the outlet dewpoint is below -70C.

B. Dry $CO_{2(g)}$ latent air input and $CO_{2(g)}$ meters

Dry cabin air was generated via a compressor that took room air and fed it to a commercially available Pressure Swing Adsorption (PSA)(Twin Tower model HR7). PSA air entered at 30SCFM and controlled via a MFC (Alicat MCR Series). The $CO_{2(g)}$ is fed from a UHP $CO_{2(g)}$ cylinder (Matheson Tri-Gas). The $CO_{2(g)}$ concentration was maintained at 2600 +/-50ppm by the feedback loop between the $CO_{2(g)}$ meter (LiCOR 840A) and the MFC (MKS 1959A). Another $CO_{2(g)}$ meter (Sable CA-10: 0-20000ppm) measured the $CO_{2(g)}$ at the exit of stage 1.

At the exit of stage 2,there was a h $CO_{2(g)}$ meter (CO2 meter CM-0052, 50-100%CO2) that measured the $CO_{2(g)}$ concentration when stage 2 A/B was delivering. The CM-0052 meter measures $CO_{2(g)}$ concentration near 100%. In addition, at stage 2 exit, a syringe sampling system was also set up to take spot samples for analysis on the gas chromatograph (HP Series II 5890).

C. Instrumentation and valves

Valves between stage 1A(or 1B) an stage 2B (or 2A) were opened only when the pressure in stage 2B (or 2A) was higher (above 3psia) than that of stage 1A (or 1B). This was when one adsorbent bed delivers to the TSAC (stage 2) bed of the other canister. Product delivery from stage 2 was controlled via a pressure transducer. When the pressure in stage 2 was above 20psia, the stage 2 valve opened and the MFM (Alicat MCR Series) measured the exit flow rate.

D. Heater control

Throughout stage 1 there were one RTD sensors on each of the six helical heaters and 12 RTD sensors embedded on the sorbent materials. The RTDs were cemented on the heater surface or cemented on alumnina rods that is fixed within the heater helix structure. RTD were placed strategically throughout the vertical, horizontal, and radial direction so that temperature uniformity and flow patterns can be monitored. During operation, the heaters are controlled through a solid state relay with 280˚C temperature set-point. The RTD heaters readings were chosen as the heaters control temperatures. This is done to avoid the overheating and scorching of the sorbents that are touching or located near the heaters coils. During air save, a vacumn pump pulled stage 1 vacuum down to 50mTorr

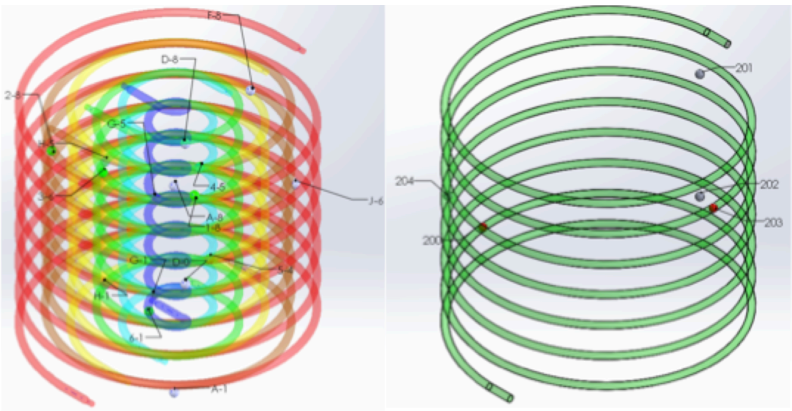

Figure 9: RTD location strategically placed through the sorbent beds; (left) stage 1 and (right) stage 2

E. Cycle control

The integrated system was automated via National Instrument Data Acquisition Hardware (cRIO 9022 and C Modules) and the CRCS LabView program. The program control the cycle time, valves, heaters, MFCs, and other associated instrumentation according to the operation scheme outlined in Table 3.

V. Results and Discussion

Many integrated runs were completed with 30scfm PSA air and 2600ppm $CO_{2(g)}$ input into stage 1A/B. Mass flow rate, temperatures, $CO_{2(g)}$ concentration, and pressure readings were recorded. Unfortunately, there were two major modes of failures.

One, the canister valve lids stage 1 failed repeatedly for both bed A and bed B when the o-rings around the lids broke. This is a failed valve design. Several possible cause to these failures are discussed here. The heating cycle (from bake-out procedures and/or the regeneration) and the air save mode may have sealed the o-ring too tight on the lids. Therefore, when the valve plate was opened, the o-ring adhered to the lids inself instead of remaining on the valve plate. The valves were opened and closed using the pneumatically operated air cyclinders set a 50psig. Although the opening and closing of the valves were observed to ensure slow movements, it is unclear if the cyclic operation may have changed these conditions. It may be that the pneumatic air-operated valve system is not a good choice and other methods of valve control is necessary (e.g. ball screws). In addition, initially, the sealing mechanism around the circular valve was a "u-shaped" type o-ring. After fabrication, this shape was determined to be insufficient as it failed to create a vacuum seal. Therefore, a circular o-rings was designed into the current o-ring grooves. Eventhough the circular o-rings were custom fabricated high temperature Kalrez o-ring, the o-rings themselves may not be fitted well with the current o-rings grooves as these grooves were deisned for u-shaped o-rings.. Many different O-ring lubricants were used to fix the failed valves, but none worked. Perhaps a dovetail o-ring groove would be better suited for this application. These failures are still under investigation.

Two, stage 1 sorbent in both canisters were damaged and early $CO_{2(g)}$ breakthrough was observed. The damaged sorbent may be related to the valve failure. When the valve failed, humid air was allowed to enter the canister, thereby water was adsorbed onto the sorbent. During the normal operating cycle, it is assumed that the sorbent is free of water. Therefore, the LabView program will heat the sorbent as fast it can to reach the desired temperature. If water is on the sorbent, there could be hydrothermal damage to the sorbent, especially when temperature uniformity in the beds were poor. For future test, the LabView program will be modified such that when the valve fails, the system will shut-down and the bake-out procedure initiated.

Due to the stage 1 failures, $CO_{2(b)}$ desorbing from stage 1 to stage 2 of the integrated system did not meet expectation. As a results, the integrated system was then run in the TSAC mode only (stage 2 function) as a proof of concept that the shared wall between stage 1 and stage 2 will lead to a decrease in power consumption.

In the TSAC mode, the CRCS were allowed to operate normally in 60 minutes half-cycles. To simulate stage 1A/B operation, concentrated $CO_{2(g)}$ (Matheson) is fed into stage 2A/B via a mass flow controller. Figure 10 shows the graphs of the $CO_{2(g)}$ input flow rate (sccm) and the $CO_{2(g)}$ production rate (sccm) versus run time. The yellow and blue sections indicate which CRCS stage 2 beds (bed A or bed B) are producing. From this graph, if 1500sccm of $CO_{2(g)}$ is input in one half-cycle, 1500sccm is output in the next half cycle when the bed is heated.

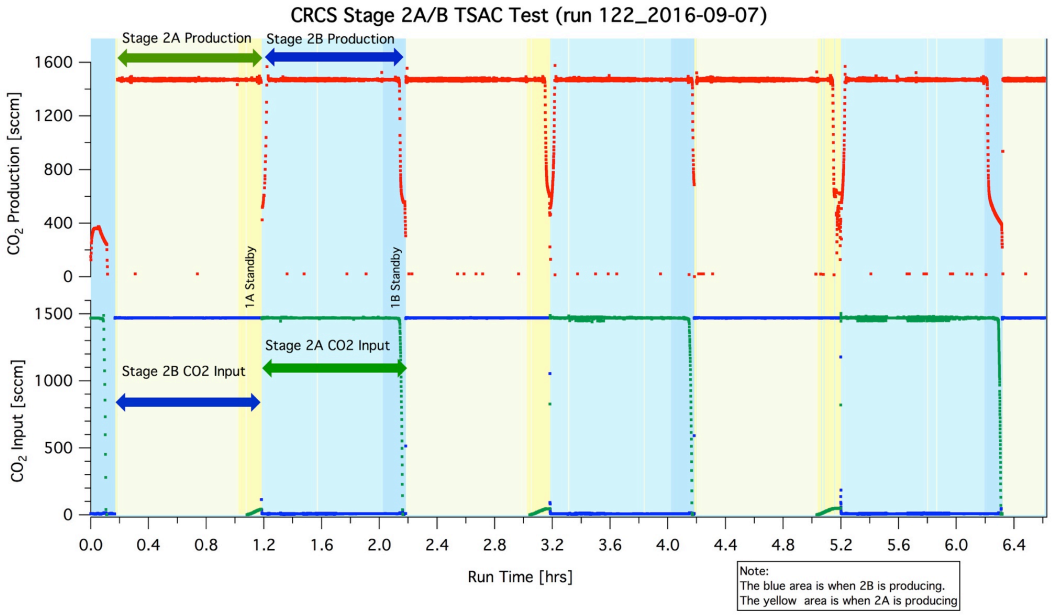

Figure 10: The graph of stage 2 CO2 input flow rate [sccm] and CO2 production rate from stage 2 versus run time [hrs]

To confirm the purity of the $CO_{2(g)}$ flow stream, a $CO_{2(g)}$ meter was placed at the exit of stage 2. Figure 11 shows stage 2A/B exit flow rate and the CO_2 concentration, in percent. The exit $CO_{2(g)}$ concentration was >99% pure indicating that there were no significant water contaminant in stage 2 that contributed to the total exit flow rate. Samples were also taken at stage 2 exit port and analyzed for $CO_{2(g)}$ in the ARC analytical lab. The lab results confirmed that the exit port air streams has >99% $CO_{2(g)}$. The CRCS stage 2 results show similar behavior to those of the AC-TSAC-2000, as expected. This validates the CRCS stage 2 functionality.

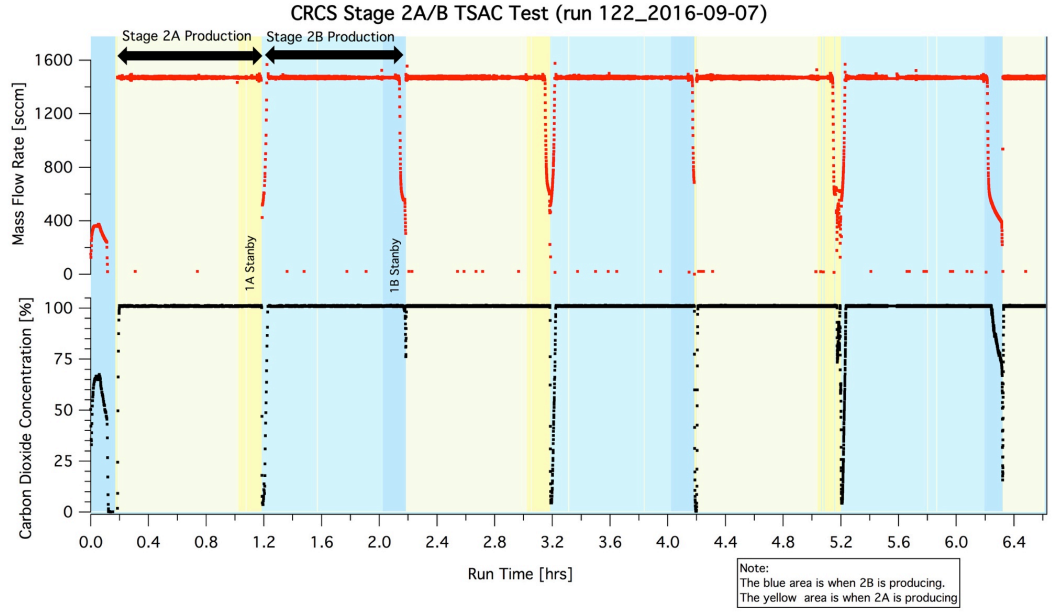

Figure 11: Graphs showing the CO2 exit flow rate [sccm] and CO2 concentration [%] versus run time.

For the gate review, the TSAC portion, or stage 2 of the CRCS was renamed the Thermally-Coupled TSAC (TC-TSAC). Isolating the TC-TSAC components from the CRCS, the mass, volume, and power number were calculated. Figure 12 shows the picture of the TC-TSAC function compared to the current Carbon Management System (CMS) and the TC-TSAC components used in the mass, volume, and power calculation for the CO2 gate review. Table 1 shows the mass, volume, and power comparison between the 4BMSX with the mechanical compressor and the 4BMS-X with the TC-TSAC. The 4BMS-X and the TC-TSAC use less power (191Watts) than the 4BMS-X and the mechanical compressors (287Watts). Therefore, the CRCS shared wall does reduce the overall power needed to heat the TSAC portion of the CRCS.

In addition, although the TC-TSAC caniter walls are stainless steel, their mass is less than the 4BMS-X. The TC-TSAC total mass is only 80lb_m mass compared to the mechanical compressor (125lb_m). It is also noted that the inner stage 2 wall is the adsorbent bed wall in the 4BMS-X. The TC-TSAC was not tested for dynamic $CO_{2(g)}$ feed conditions. Therefore, the buffer or $CO_{2(g)}$ storage cylinders (tankage) were added for completeness.

In summary, the TC-TSAC showed improve mass and power values compared to the mechanical compressor currently in use on ISS. If the CRCS heater were re-designed, the power number may improve futher.

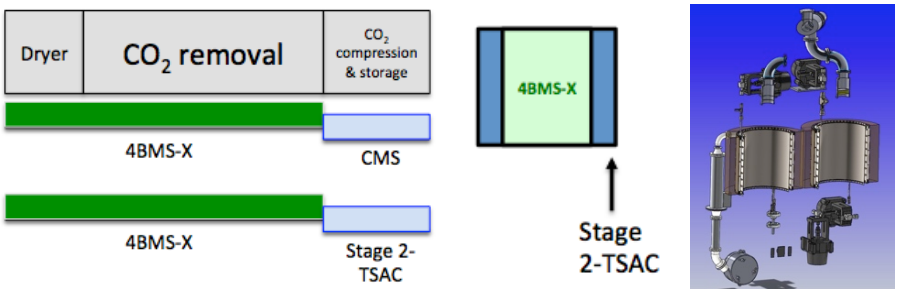

Figure 12: (left) A chart showing the function of the TC-TSAC with the Carbon Management System (CMS); (middle) a cross section if the CRCS bed stage 1 and Stage 2; (right) A cut-out of CRCS bed showing the components used to calculate the mass, volume, and power.

Table 4: The table showing the mass, volume, and power calculations for the CRCS TC-TSAC.

	Bottoms up est.	Knox spread sheet		
	Mass (lbm)	Mass(lbm)	Power (w)	Volume(ft^3)
4BMSX total	193		TBD	TBD
Mechanical compressor from CMS	125		287	
tankage from CMS	40			
4BMS-X with CMS total	**358**	**358**	**287**	
4BMSX total	193		TBD	TBD
TC -TSAC both units	88		191	
tankage (sorbent buffer)	10			
4BMS-X with TC-TSAC total	**291**	**225**	**191**	

VI. Conclusion and Future Work

The integrated CRCS system was successfully fabricated, assembled, and tested in continuous 60-minute half-cycles with 2600ppm $CO_{2(g)}$ input and measuring $CO_{2(g)}$ output. The Stage 1 valves and sorbent failed and a full failure analysis has not been completed. However, as a proof of concept, the CRCS was operated in the TC-TSAC mode. Stage 2 successfully delivery >99% pure $CO_{2(g)}$ at 4 kg/day using 191 Watts of power. Data were presented at the 2016 CO2 Gate Review. These data showed that the TC-TSAC showed both mass and power savings. There are many lessons learned from this work and future work will involve the following suggested modifications:

1. Eliminate the embedded valve design and use external valves for stage 1.
2. Add additional power feedthroughs such that the internal heaters could be individually controlled.
3. Choose another stage 2 sorbent since the current one used is no longer available commercially.
4. Redesign stage 1 heaters so that temperature uniformity within stage one can be achieved.

Acknowledgement

Acknowledgement are given to the people who first started this project: Lila Mulloth, Mini Varguese and Bernie Luna. The CRCS project is funded under the Advanced Exploration System (AES) program and we appreciate the program managers, Walter Scheiner and Sarah Schull, for their support. We also extend our appreciation to the Bioengineering branch personel, Mark Kliss and Marilyn Murakami, who assisted us in various functions. We also thank Mark Silvera from the ARC Analytical Laboratory and Brian Malone from Facilities. The following interns also helped with the various development and test: Robert Bohrer, David Marson, and Serena Le.

References

1. Frisbee, R.H., *Mass and power estimates for Mars in-situ propellant production systems*. 23rd Joint Propulsion Conference, 1987. **23**(23).
2. Mulloth, L.M. and J.E. Finn, *A solid-state compressor for integration of CO 2 removal and reduction assemblies*. 2000, SAE Technical Paper.
3. Finn, J.E., L.M. Mulloth, and B.A. Borchers, *Performance of Adsorption-Based CO 2 Acquisition Hardware for Mars ISRU*. 2000, SAE Technical Paper.
4. Mulloth, L.M. and D.L. Affleck, *Development of a Temperature-Swing Adsorption Compressor for Carbon Dioxide*. 2003, SAE Technical Paper.
5. Varghese, M., et al. *Development Status of a Low-Power CO2 Removal and Compression System for Closed-Loop Air Revitalization*. in *40th International Conference on Environmental Systems*. 2010.
6. Mulloth, L.M., et al., *Performance Characterization of a Temperature-Swing Adsorption Compressor for Closed-Loop Air Revitalization Based on Integrated Tests with Carbon Dioxide Removal and Reduction Assemblies*. 2006, SAE Technical Paper.
7. Hogan, J., et al. *The Low-Power CO2 Removal and Compression System: Design Advances and Development Status*. in *42nd International Conference on Environmental Systems*. 2012.
8. Hogan, J., et al. *Development and Testing of a Two-Stage Air Drying System for Spacecraft Cabin CO2 Removal Systems*. 2014. 44th International Conference on Environmental Systems.
9. Knox, J., et al. *Development of Carbon Dioxide Removal Systems for Advanced Exploration Systems 2012-2013*. in *43rd International Conference on Environmental Systems*. 2013.
10. Richardson, T.-M.J., et al. *Progress on the CO2 Removal and Compression System*. 2015. 45th International Conference on Environmental Systems.
11. Richardson, T.-M.J., et al. *Integrated CO2 Removal and Compression System Performance*. 2016. 46th International Conference on Environmental Systems.
12. Moate, J.R., *Temperature swing adsorption compression and membrane separations*. 2009, Vanderbilt University.